

## ORIGINAL ARTICLE

# Quasi-static acoustic tweezing thromboelastometry

R. G. HOLT,\* D. LUO,† N. GRUVER\* and D. B. KHISMATULLIN†\*

\*Department of Mechanical Engineering, Boston University, Boston, MA; and †Department of Biomedical Engineering, Tulane University, New Orleans, LA, USA

**To cite this article:** Holt RG, Luo D, Gruver N, Khismatullin DB. Quasi-static acoustic tweezing thromboelastometry. *J Thromb Haemost* 2017; 15: 1453–62.

## Essentials

- Blood coagulation measurement during contact with an artificial surface leads to unreliable data.
- Acoustic tweezing thromboelastometry is a novel non-contact method for coagulation monitoring.
- This method detects differences in the blood coagulation state within 10 min.
- Coagulation data were obtained using a much smaller sample volume (4  $\mu$ L) than currently used.

**Summary.** *Background:* Thromboelastography is widely used as a tool to assess the coagulation status of critical care patients. It allows observation of changes in material properties of whole blood, beginning with early stages of clot formation and ending with clot lysis. However, the contact activation of the coagulation cascade at surfaces of thromboelastographic systems leads to inherent variability and unreliability in predicting bleeding or thrombosis risks. *Objectives:* To develop acoustic tweezing thromboelastometry as a non-contact method for perioperative assessment of blood coagulation. *Methods:* Acoustic tweezing is used to levitate microliter drops of biopolymer and human blood samples. By quasi-statically changing the acoustic pressure we control the sample drop location and deformation. Sample size, deformation and location are determined by digital imaging at each pressure. *Results:* Simple Newtonian liquid solutions maintain a constant, reversible location vs. deformation curve. In contrast, the location/deformation curves for gelatin, alginate, whole blood and blood plasma uniquely change as the samples solidify. Increasing elasticity causes the sample to deform less, leading to steeper stress/strain curves. By

extracting a linear regime slope, we show that whole blood or blood plasma exhibits a unique slope profile as it begins to clot. By exposing blood samples to pro- or antithrombotic agents, the slope profile changes, allowing detection of hyper- or hypocoagulable states. *Conclusions:* We demonstrate that quasi-static acoustic tweezing can yield information about clotting onset, maturation and strength. The advantages of small sample size, non-contact and rapid measurement make this technique desirable for real-time monitoring of blood coagulation.

**Keywords:** acoustics; biopolymers; blood coagulation tests; rheology; whole-blood coagulation time.

## Introduction

The depletion of both pro- and anticoagulants and other alterations in the coagulation system, known generically as coagulopathy, often develop as a result of: a significant blood loss during trauma, major surgery or post-partum hemorrhage; extracorporeal blood flow during cardiopulmonary bypass or hemodialysis; or disseminated intravascular coagulation caused by systemic activation of the coagulation system in sepsis and cancer. Coagulopathic patients are at high risk of both bleeding and thrombotic complications and require perioperative monitoring of their coagulation status. Plasma coagulation assays (e.g. prothrombin time [PT] and activated partial thromboplastin time [APTT]), are a standard way to monitor for coagulation disorders. However, they have low predictive power in patients with coagulopathy [1]. In this situation, the use of whole-blood coagulation tests becomes important.

Contact ‘pin-and-cup’ methods such as thromboelastography (TEG), rotational thromboelastometry (ROTEM) and Sonoclot are currently available to measure the coagulation status of whole blood [2–4]. These methods measure temporal changes in the shear force between a disposable cup containing a 0.3–0.4 mL sample of whole blood and a pin immersed in the blood sample. Intrinsic pathway activators such as kaolin or ellagic acid are required to initiate coagulation using this approach. The ‘pin-and-cup’ techniques accurately diagnose hyperfibrinolysis and are

Correspondence: Damir B. Khismatullin, Department of Biomedical Engineering, Tulane University, 6823 St. Charles Avenue, New Orleans, LA 70118, USA.  
Tel.: +1 504 247 1587.  
E-mail: damir@tulane.edu

Received 1 September 2016

Manuscript handled by: S. Kitchen

Final decision: P. H. Reitsma, 24 April 2017

helpful but not reliable tools in screening for hypercoagulable states and transfusion guidance [5]. However, the contact of a blood sample with the pin and cup surfaces creates artificial conditions for blood coagulation, leading to substantial differences from the dynamics of hemostasis in the body. This inherent deficiency is an important reason for the poor standardization and high variability of these methods [6], their inability to determine disorders of primary hemostasis [7], their unreliability in detection of impaired platelet function [8] and prediction of bleeding after major surgery [9], and a strong effect of heparin flush on thromboelastographic parameters leading to the necessity of discarding a large volume of blood before measurement [10]. Even with intrinsic pathway activators present, the coagulation process occurring in 'pin-and-cup' devices remains slow. A significant amount of time (30–60 min) is required to obtain the results needed for diagnosis unless the extrinsic pathway activators (e.g. tissue factor) are used [3,11] or the disease state can be detected using only early parameters such as reaction and kinetic times.

Employing a container less (air-contact) processing technique would eliminate the problems alluded to above. Ultrasonic acoustic levitation has been widely utilized for processing of container less materials [12–18]. Its low interference with samples and relative simplicity, along with its ability to quasi-statically or dynamically deform the sample with no contact, make it a desirable candidate for rheological applications [14–16,19]. In the present study the quasi-static technique, referred to as 'quasi-static acoustic tweezing thromboelastometry' (QATT), is employed to measure rheology of biological gels and human blood.

## Materials and methods

### *Reagents and solutions*

In the proof-of-concept experiments, three gel mixtures were used: 2 000 000-MW dextran from *Leuconostoc* spp. (Sigma-Aldrich, St. Louis, MO, USA), 300-bloom gelatin from porcine skin (Sigma-Aldrich), and sodium alginate (Sigma-Aldrich). Gel solutions were prepared by hydrating dextran, gelatin or sodium alginate in a small amount of distilled water for 10 min, then adding boiling distilled water to achieve the desired concentration. Calcium carbonate  $\text{CaCO}_3$  (Sigma-Aldrich) in combination with 6% (w/w) D-(+)-Gluconic acid  $\delta$ -lactone (GDL, Sigma-Aldrich) was used as a source of calcium ions to initiate gelation of sodium alginate. The molar ratio of a basic calcium ion to carboxyl was kept at 0.36. The sodium alginate solution was mixed and vortexed with the  $\text{CaCO}_3$  suspension for 1 min. A fresh aqueous GDL solution was then added to the resulting mixture to initiate gelation.

In the whole blood studies, cytochalasin D (Sigma-Aldrich) dissolved in phosphate-buffered saline (PBS, Thermo Fisher Scientific, Waltham, MA, USA) was used

as an antiplatelet agent. Cytochalasin D inhibits platelet function by blocking polymerization of actin filaments. It is used in ROTEM to measure the functional level of fibrinogen and diagnose fibrin/fibrinogen deficiency [20]. Recombinant human tissue factor (TF, R&D Systems, Minneapolis, MN, USA) in PBS was used as a procoagulant. In the blood plasma studies, human fibrinogen (Enzyme Research Laboratories, South Bend, IN, USA) and Gly-Pro-Arg-Pro (GPRP, Sigma-Aldrich), both dissolved in PBS, were used as pro- and antithrombotic agents, respectively.

### *Preparation of blood samples*

Whole blood samples were collected from 30 healthy male and female volunteers with age ranging from 22 to 39 years using protocol 520566-13 approved by the Institutional Review Board of Tulane University. Each volunteer donated 29.9 mL blood, which was transferred into vacutainer tubes (BD, Franklin Lakes, NY, USA) containing sodium citrate (blue cap, one 4.5-mL tube and two 2.7-mL tubes), EDTA (pink cap, three 6-mL tubes) or K2EDTA (purple cap, one 2.0-mL tube). One blue-cap and one purple-cap tube were used for standard coagulation tests (PT, international normalized ratio [INR], APTT, fibrinogen and platelet concentration) conducted at the Coagulation Laboratory of Tulane University Hospital. The remaining tubes were used in acoustic tweezing experiments.

For half of the experiments no pretreatment to initiate coagulation of the collected blood (whether citrated or EDTA-treated) was carried out. For the remaining experiments, 180  $\mu\text{L}$  of citrated- or EDTA-treated blood was mixed with 20  $\mu\text{L}$  of 0.2 M calcium chloride  $\text{CaCl}_2$  (Sigma-Aldrich) within 4 h of blood collection to start the coagulation cascade. To test the effect of coagulation activators or antiplatelet agents, 16 EDTA-treated blood samples were mixed, respectively, with TF (eight samples) or cytochalasin D (eight samples) 10 min before the sample re-calcification. The final concentration of TF and cytochalasin D in blood was  $13 \text{ pg mL}^{-1}$  and  $7.6 \text{ } \mu\text{g mL}^{-1}$ , respectively. Immediately after pretreatment, a 4- $\mu\text{L}$  drop was deployed into the tweezing apparatus to begin the deformation experiment. This process was repeated until the desired number of experiments was performed.

Commercial factor assay control plasma (FACT), which is citrated blood plasma pooled from 30 or more normal human donors, was purchased from George King Bio-Medical (Overland Park, KS, USA); 300  $\mu\text{L}$  aliquots of FACT were stored at  $-80^\circ\text{C}$ . To initiate coagulation, the aliquots were thawed in a  $37^\circ\text{C}$  water bath and then mixed with 0.2 M  $\text{CaCl}_2$  (22.5  $\mu\text{L}$  of FACT per 2.5  $\mu\text{L}$   $\text{CaCl}_2$ ) immediately before tweezing. To determine the effect of pro- or antithrombotic agents on plasma coagulation, FACT samples were mixed with fibrinogen or GPRP

10 min before the re-calcification procedure. The final concentration of fibrinogen in plasma, accounting for the intrinsic concentration of fibrinogen ( $269 \text{ mg dL}^{-1}$ ), was  $610 \text{ mg dL}^{-1}$ . Note that the normal range for fibrinogen concentration is  $150\text{--}400 \text{ mg dL}^{-1}$  [21]. The GPRP concentration was  $340 \text{ mg dL}^{-1}$  (8 mM).

#### Acoustic tweezing apparatus and quasi-static technique

The apparatus for acoustic tweezing, also known as an acoustic levitator, was custom fabricated. Figure 1(A) shows a schematic of the electrical and mechanical systems used to levitate samples. The transducer consists of two 3.175-mm-thick piezoelectric discs (Channel Industries, Santa Barbara, CA, USA) and aluminum bottom mass and horn. The working frequency of the transducer is nominally 30 kHz, requiring slight retuning to compensate for temperature shifts. The transducer and the reflector (an aluminum cylinder) were mounted either a full or half wavelength apart, and the assembly could be optionally inserted into a custom fabricated and sealed environmental chamber for pressure, temperature and humidity control or a 3-D positioning system custom built using parts bought from Thorlabs (Newton, NJ, USA).

The 30-kHz sinusoidal input signal was generated by a function synthesizer (Agilent 33220A, Santa Clara, CA, USA) and amplified (Krohn-Hite 7500, Brockton, MA, USA) before being sent to the transducer; the resulting

vibration creates an acoustic standing wave in the air gap between the transducer and the reflector.

QATT focuses on the deformed shapes that samples take when subjected to an acoustic pressure varying slowly enough to maintain mechanical equilibrium. In a typical experiment, a sample drop is levitated and the simultaneous vertical location and drop shape deformation (aspect ratio) are obtained via imaging. The technique relies on the fact that, as the acoustic pressure amplitude changes (pressure sweep) but remains relatively low, the location and aspect ratio of a sample drop are uniquely determined by its material properties and size. The pressure sweep is completed in 30 s or less, which is much shorter than blood clotting time. When the pressure amplitude is low, the gravity-controlled limit is reached at which the drop location changes appreciably. In this limit, the location is a measure of the acoustic stress applied to the drop to lift it, whereas the aspect ratio is a measure of the strain resulting from the applied acoustic stress. Therefore, within this limit, a location vs. aspect ratio curve represents an effective stress/strain curve for a given material.

#### Experimental procedure

Samples ( $4 \mu\text{L}$  nominally) were deployed manually into a node of the standing wave using a gastight  $100\text{-}\mu\text{L}$  glass syringe (Hamilton 7656, Reno, NV, USA) with a polytetrafluoroethylene-coated stainless steel blunt-tipped needle

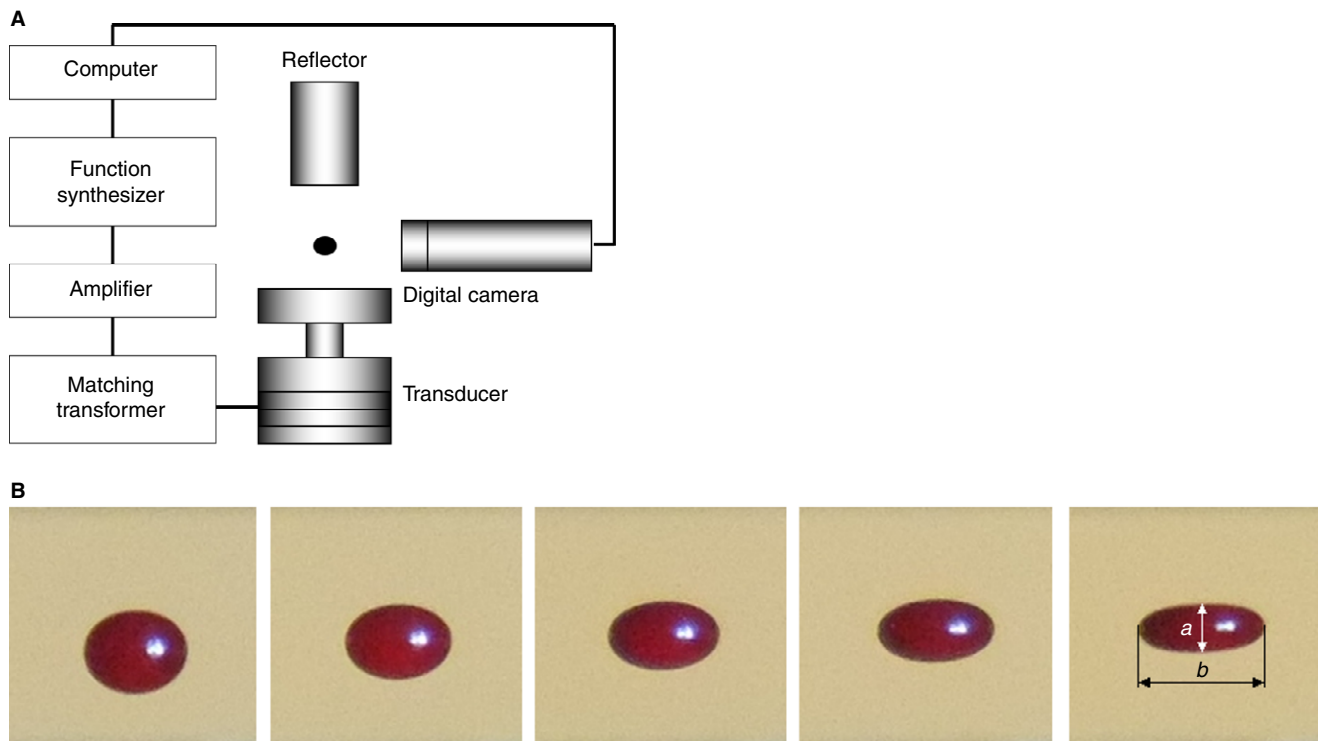


**Fig. 1.** (A) Schematic of the acoustic tweezing device. (B) Sequence of photos of a whole blood sample levitating in the device under increasing acoustic pressure (from left to right). The levitator frequency was 29.4 kHz, the field of view of each image is  $5 \text{ mm} \times 5 \text{ mm}$ , and the elapsed time between images is 3 s. [Color figure can be viewed at [wileyonlinelibrary.com](http://wileyonlinelibrary.com)]

(Hamilton 8646). Every experiment began with tuning the transducer to near resonance and then injecting a sample into a standing wave node. Sample deformation was induced by varying the standing wave pressure amplitude. This was accomplished either by varying the amplifier input voltage at a fixed frequency, or by varying the frequency at a fixed voltage input. Sample images were obtained by a Retiga 1300 digital camera (QImaging, Surrey, Canada) or an acA1920-25um camera (Basler, Ahrensburg, Germany) at regular intervals. The spatial resolution of the images was 0.012 mm. Figure 1(B) shows typical shapes of a whole blood sample during an acoustic tweezing experiment. As seen in this figure, an increase in the deformation of the sample correlates with an increase in its vertical position.

#### *Quantification of drop size, deformation and location*

Location and shape deformation of tweezing samples were obtained by analyzing the image sequences using a custom program written in MATLAB (Mathworks, Natick, MA), which relied on the MATLAB image processing toolbox. The analysis began with edge detection using a modified Canny method [22]. The 'blob analysis' tools within MATLAB were then used to find the centroid of the drop and quantify deformation as an aspect ratio (width  $b$ /height  $a$ , cf. Fig. 1B). Location was measured as a vertical distance from the sample centroid to a fixed location on the apparatus. Slopes of the initial portion of location vs. aspect ratio curves were obtained by linear regression and quantified by calculating the angle of inclination to the horizontal (aspect ratio) axis. Hence, for a line of slope  $m$ , we refer to an angle  $\theta = \arctan(m)$ . For convenience, we refer to the slope angle vs. time curves (Figs 3D, 5, 6A, 7A) as 'tweezographs'. Some of the tweezographs (Fig. 7A) have been normalized based on  $\theta_0$ , the slope angle at time 0.

#### *Statistical analysis*

Twenty-five volunteers' data were analyzed for the results reported in Figs 1, 5 and 6. Twelve to fifteen volunteers' blood samples were subject to TF and cytochalasin D, as reported in Fig. 6. The results were evaluated with  $t$ -test and ANOVA using GraphPad Prism version 5.0.2 (GraphPad Software, La Jolla, CA, USA). The statistical data were presented as mean  $\pm$  standard error of the mean (SEM). Statistically significant differences were set at  $P < 0.05$  (95% confidence).

## **Results**

### *Newtonian fluids*

Generally, for viscoelastic fluids such as human blood, the sample's drop shape is a function of bulk viscosity and elasticity. These two properties have different time profiles

during coagulation, potentially complicating the analysis and interpretation of raw measurement data. Blood coagulation is associated with an increase in blood elasticity (firmness), but its effect on blood viscosity is less clear and most likely transient. Thus, for coagulation analysis, it is desirable to have an elastometric technique, which is highly sensitive to changes in blood elasticity but not blood viscosity. To test whether QATT satisfies this requirement, we first conducted experiments with a dextran-in-water solution. This solution is a non-reacting Newtonian fluid [23] in which the bulk viscosity increases with polymer concentration, the bulk elasticity is zero and the restoring force for deformation is just the surface tension. As seen in Fig. 2(A), the aspect ratio vs. location curves of 5% dextran solution remain constant and reversible during 10 min of acoustic tweezing. The solution concentration has a negligible effect on the curves (Fig. 2B), indicating that QATT is insensitive to changes in bulk viscosity.

A very different behavior is seen when the material under study undergoes a state change from a liquid to a solid. When gelatin or alginate are diluted in water, they form hydrogels characterized by much higher bulk elasticity than the initial solutions of these polymers. The location vs. aspect ratio curves plotted in Fig. 3 demonstrate that QATT is sensitive to changes in bulk elasticity occurring during gelation of these materials. For both gelatin and alginate, the sample location increases approximately linearly with aspect ratio until breaching the gravity-controlled limit. Beyond this limit, the drop deforms more readily without much changes in its location. In the linear regime, the slope of the location vs. aspect ratio curve for gelatin increases with time until 13 min later, when the sample is fully gelled (Fig. 3A). Figure 3(B) shows the concentration dependence of gelatin drops at 2 min into an experiment, when they are partially gelled. The slope in the linear region of the location vs. aspect ratio curves increases with increasing gelatin concentration. Alginate, in contrast to porcine gelatin, will not gel without exposure to calcium ions. Thus, it behaves similar to citrated or EDTA-treated blood, which do not coagulate until exposure to calcium ions (re-calcification). Figure 3(C) shows the location vs. aspect ratio curves for alginate at selected times up to 34 min after initiation of gelation by a GDL solution. The linear response region is restricted to the data in the bounding box in the lower left corner of Fig. 3(C). After performing linear regression on the data in the box, where the location is well within the gravity-controlled limit, we obtained the 'tweezograph' (Fig. 3D), which plots the linear slope angle  $\theta$  vs. time. From the tweezograph we can clearly detect changes in gel firmness, as quantified by angle  $\theta$ , because of an increase in polymer concentration. Additionally, we see that the firmness dramatically increases for 4% alginate at about 4 min after the alginate drop injection into the acoustic tweezing device. After about 14 min,  $\theta$  begins to level off with increasing time, indicating the approach to



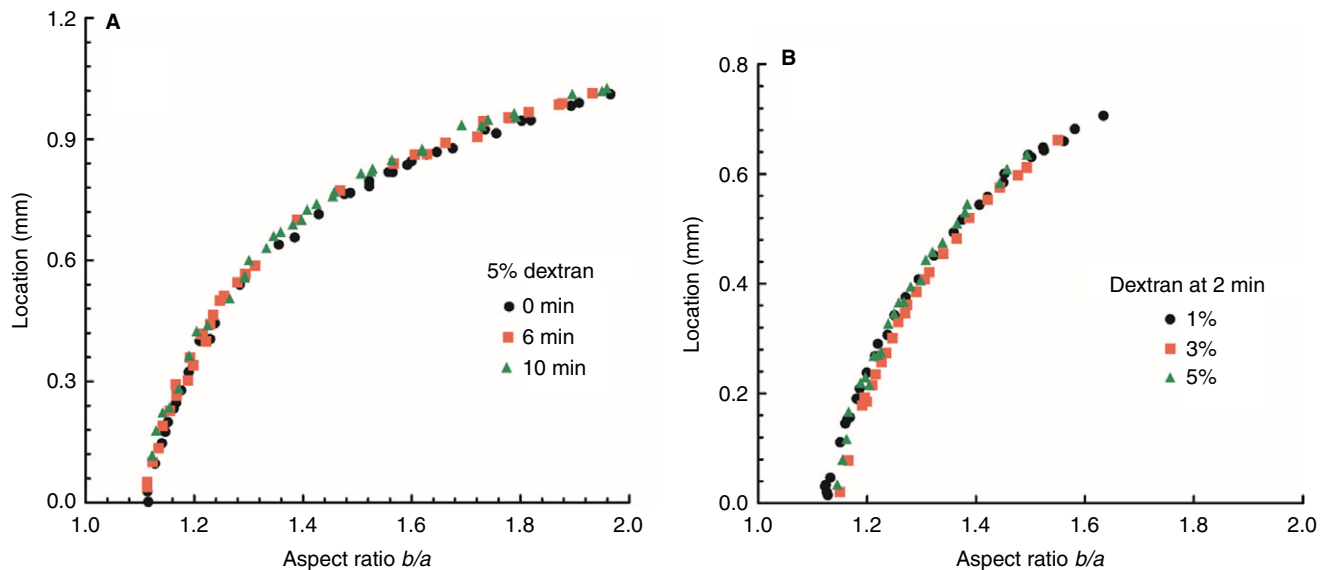


**Fig. 2.** Location vs. aspect ratio for dextran samples obtained by increasing and decreasing pressure amplitude. (A) A 0.95-mm radius drop of 5% dextran at 0, 6 and 10 min. (B) Single drops of 1%, 3% and 5% dextran at 2 min. The drop radii were nominally 0.95 mm. [Color figure can be viewed at [wileyonlinelibrary.com](http://wileyonlinelibrary.com)]

the fully gelled state. We identify these three distinct regions as Stage I (initial gelation or coagulation), Stage II (rapid gelation or coagulation) and Stage III (convergence to fully gelled or coagulated) in Fig. 3(D) to facilitate our discussion below. Taken together, Fig. 3 confirms that we may take  $\theta$  as a measure of the sample firmness, and the method itself is capable of measuring time-dependent changes in the firmness of reacting samples. The ‘tweezograph’ of the time dependence of  $\theta$  displays three distinct stages of clotting kinetics.

### Blood

Healthy subjects studied (13 male and 17 female) had the values of their coagulation parameters within normal ranges: PT of  $10.53 \pm 0.12$  s, INR of  $0.995 \pm 0.017$ , APTT of  $28.40 \pm 0.94$  s, fibrinogen of  $290 \pm 12$  mg dL<sup>-1</sup>, and  $260.0 \pm 8.0$  platelets mL<sup>-1</sup>.

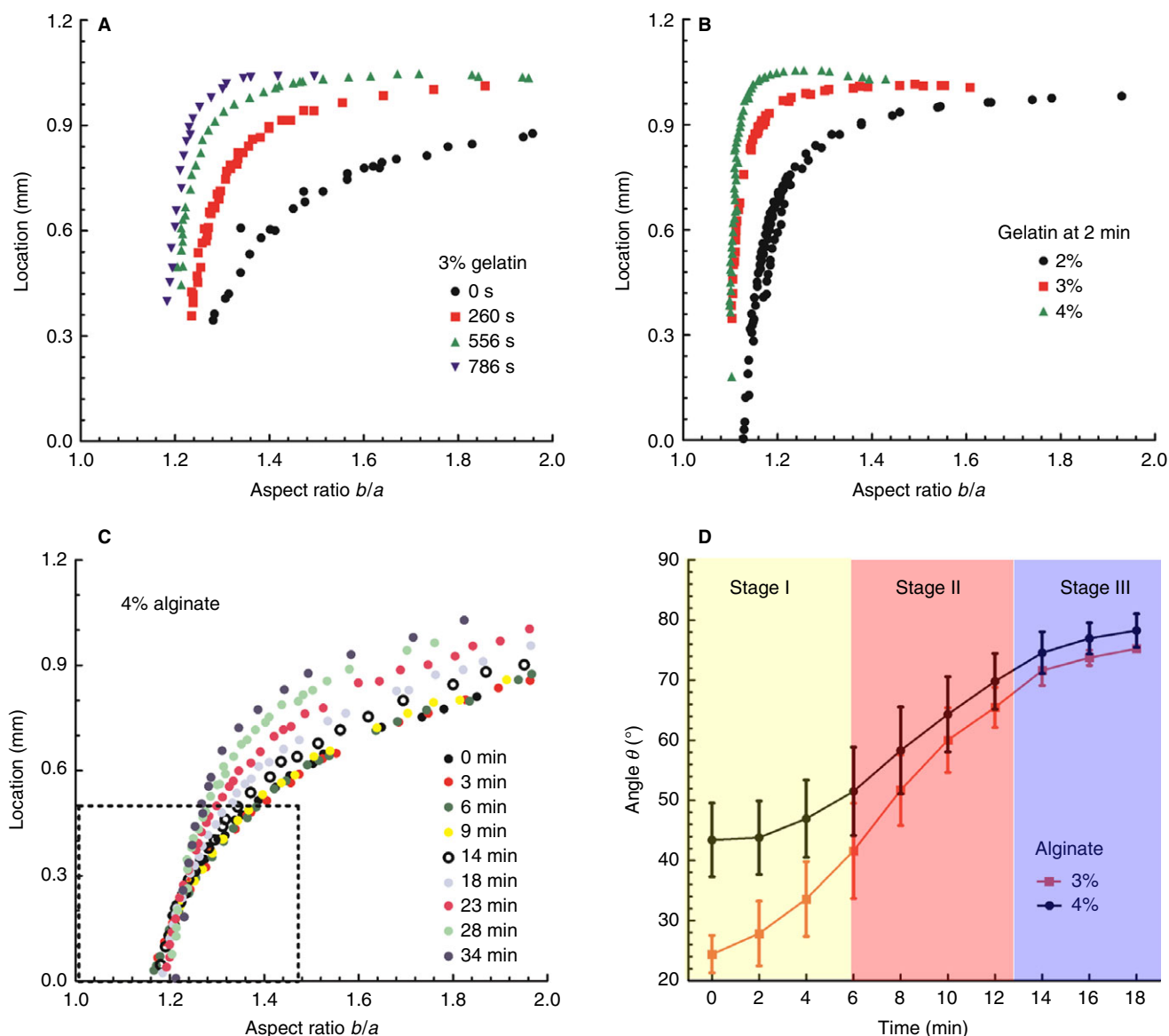
Figure 4 shows the typical aspect ratio vs. location curves for all whole blood samples. As with alginate, for short times (< 20 min) the firmness increases with time, but the drops return to the same initial deformation and location. After 20 min, the coagulated drops return to a permanently deformed state at the lowest location. As the cyclic loading and unloading process continues this permanent deformation itself continues to increase with time.

Figure 5 shows the tweezographs for citrated acid (A) and EDTA (B) treated groups. Remarkably, all the curves (except EDTA without CaCl<sub>2</sub> in Fig. 5B) show the same general features as the results for gelatin and alginate already shown in Fig. 3. At short times (Stage I),  $\theta$  starts between 52° and 56° (citrated,  $54.77 \pm 0.88$ ; citrated+CaCl<sub>2</sub>,  $55.92 \pm 1.78$ ; EDTA,  $52.83 \pm 0.53$ ;

EDTA+CaCl<sub>2</sub>,  $53.78 \pm 1.00$ ), increasing gradually as coagulation proceeds for a time whose value depends on whether the coagulation is aided by the addition of free calcium ions via introduction of CaCl<sub>2</sub>. Following this initial mild increase in firmness, there follows a period of rapid increase (Stage II) in  $\theta$ , which happens much sooner for CaCl<sub>2</sub>-exposed blood in both citrated and EDTA-treated samples. This period of rapid increase is then followed by a leveling off of the firmness increase (Stage III), approaching an asymptotic value for long times. It is noteworthy that the coagulation process converges at long times to roughly the same Stage III path, with values for  $\theta$  reaching 82°–84° (citrated,  $81.72 \pm 0.91$ ; citrated + CaCl<sub>2</sub>,  $82.20 \pm 0.38$ ; EDTA + CaCl<sub>2</sub>,  $83.51 \pm 0.52$ ) at 25 min when the experiments were halted.

Blood samples treated with EDTA without CaCl<sub>2</sub> (Fig. 5B) exhibit a prolonged Stage I slow growth in firmness. These data were only shown up to 14 min, because many of these more slowly coagulating samples developed a ‘scab’ on the surface after 14 min. Although scab formation is a natural outcome, and our method is certainly capable of detecting its formation, its presence only in the EDTA without CaCl<sub>2</sub> group makes comparison with samples without scab formation difficult.

Figure 6 illustrates the effect of TF and cytochalasin D on whole-blood coagulation in the tweezing device. Samples treated with TF are immediately stiffer (TF: initial  $\theta = 57.3 \pm 1.63^\circ$ , untreated:  $52.32 \pm 1.64^\circ$  in Fig. 6A) and, because they show almost immediate Stage II rapid growth in firmness and continue to be stiffer than the untreated group throughout the untreated group’s Stage I and II coagulation, as seen in Fig. 6(B). On the other hand, samples treated with cytochalasin D (Fig. 6C)



**Fig. 3.** Location vs. aspect ratio for porcine gelatin and alginate samples obtained by increasing and decreasing pressure amplitude. (A) 0.90-mm radius drop of 3% gelatin at increasing times. (B) 0.90, 0.89 and 0.86-mm drops of 2%, 3% and 4% gelatin at 2 min. (C) Location vs. aspect ratio curves of a 4% alginate drop with radius of 0.98 mm from 0 to 34 min. The box indicates the portion of the data for which we performed linear regression for location vs. aspect ratio to obtain  $\theta$ . (D) Tweezograph ( $\theta$  vs. time) of 4 drops (nominal radii of 0.98 mm) each of 3% and 4% alginate from 0 to 18 min. [Color figure can be viewed at [wileyonlinelibrary.com](http://wileyonlinelibrary.com)]

display a longer Stage I with a delayed onset of Stage II, and thus remain less stiff relative to the untreated group. By 25 min, both treated and untreated samples converge to a similar Stage III firmness (untreated,  $85.46 \pm 0.27^\circ$ ; TF,  $85.51 \pm 0.60^\circ$ ; cytochalasin D,  $84.79 \pm 0.49^\circ$ ).

Blood plasma samples show a similar three-phase coagulation process in their tweezographs (Fig. 7). As seen in Fig. 7(A), high fibrinogen plasma produces much stiffer clots ( $\theta/\theta_0 = 1.10$ ) than FACT ( $\theta/\theta_0 = 1.05$ ) or GPRP-treated plasma ( $\theta/\theta_0 = 1.02$ ). According to Fig. 7(B), a significant difference in clot firmness between high fibrinogen plasma and FACT was already observed at 5 min of sample tweezing (FACT,  $\theta/\theta_0 = 1.02 \pm 0.002$ ;

high fibrinogen,  $1.04 \pm 0.01$ ), whereas GPRP-treated plasma showed a significant decrease in clot firmness as compared with FACT, starting at 7 min (FACT,  $1.03 \pm 0.002$ ; GPRP,  $1.02 \pm 0.003$ ). Using FACT samples from the same batch, we observed that the coefficient of variation (CV) for 12-min QATT coagulation ( $\theta/\theta_0$ ) measurement ranged from 0.4% to 0.8%.

## Discussion

In this paper, we report the development of an acoustic tweezing technique for acquiring soft biological material properties, and its initial application to gels and blood.

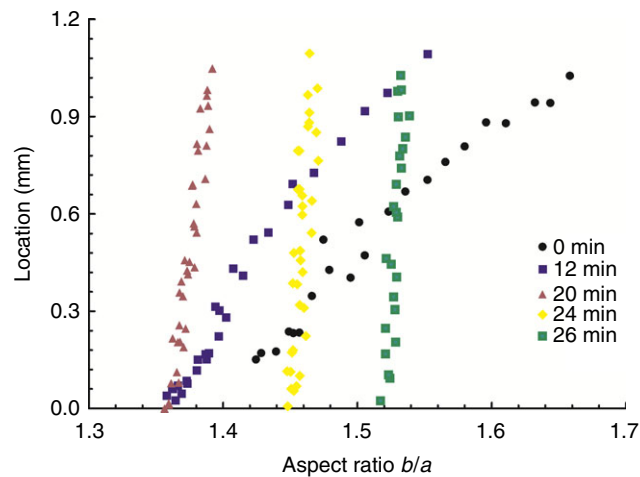


**Fig. 4.** Location vs. aspect ratio curves of a 1.0-mm radius drop of citrated whole blood at 0, 12, 20, 24 and 26 min. The blood sample was not exposed to  $\text{CaCl}_2$ . [Color figure can be viewed at [wileyonlinelibrary.com](#)]

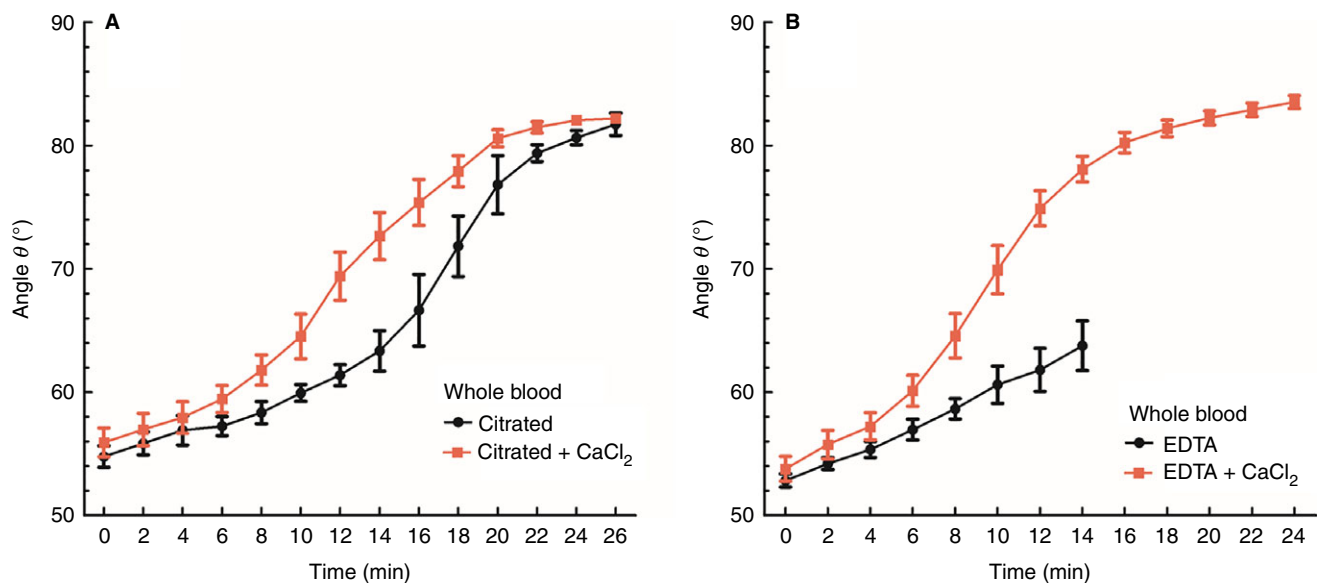


**Fig. 5.** Tweezographs of (A) 39 drops of citrated control and 47 drops of citrated +  $\text{CaCl}_2$  whole blood and (B) 44 drops of EDTA control and 50 drops of EDTA +  $\text{CaCl}_2$  whole blood. [Color figure can be viewed at [wileyonlinelibrary.com](#)]

The tweezograph analysis introduced in Figs 3 and 5 illustrates the ability of our technique to detect time-dependent changes in elasticity of soft materials as they undergo solidification or in blood as it undergoes coagulation. The results establish that  $\theta$ , the quantitative measure in the tweezograph, is robust and sensitive to the changes characteristic of such processes. When applied to whole blood (Fig. 6) or blood plasma (Fig. 7), our method can distinguish between normal, hyper and hypocoagulable states in less than 10 min.

The coagulation status of whole blood in coagulopathic patients and patients requiring blood product administration is routinely assessed by thromboelastographic tests. In these techniques, a cuvette with blood and a suspended pin are forced into oscillatory rotation (TEG, ROTEM)

or translation (Sonoclot) relative to each other. The clot that forms induces changes in the motion of the pin or cuvette, and the amplitude of the motion is plotted vs. time for both clot formation and lysis [2]. As an example, in TEG, the envelope of the peak amplitude forms a rising sigmoidal curve (the ‘trace’). The trace is initially zero when no fibrin links the pin and cup: the time from beginning of a TEG experiment to the first non-zero trace is called the ‘Reaction time’ or ‘R time’, which is a measure of the time to form a fibrin network between cup and pin, typically 5–10 min when no data are obtained from TEG. The apparent amplitude at long times (‘MA’ in TEG) is a measure of firmness, and the rise to MA is characterized by its angle with the horizontal time axis (‘angle  $\alpha$ ’ in TEG) at a chosen value (22 mm in TEG) of

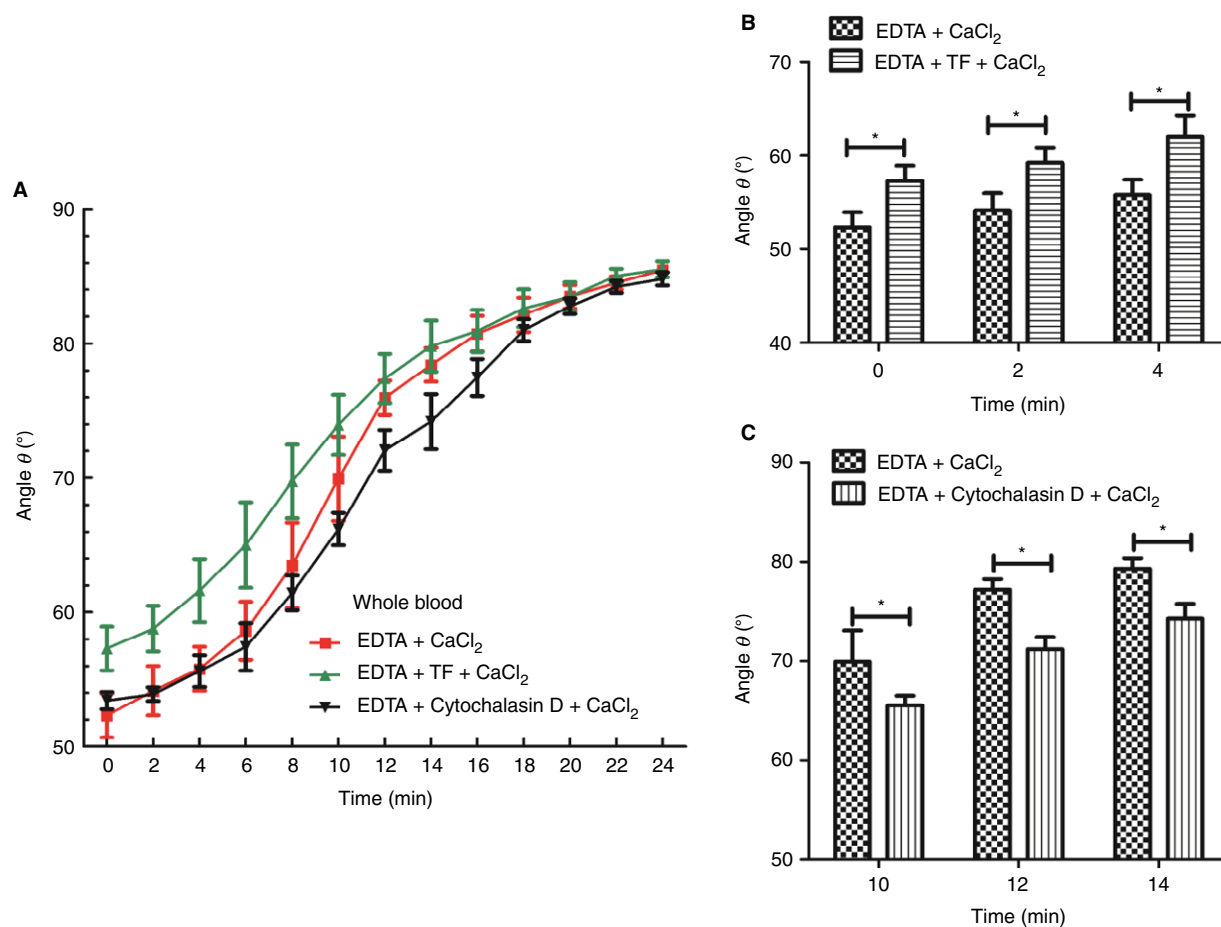


**Fig. 6.** (A) Tweezographs of EDTA-treated whole blood with added  $\text{CaCl}_2$  and exposed to 0.9% saline (8 drops), tissue factor (TF) (8 drops) or cytochalasin D (8 drops). (B) Effect of TF on  $\theta$  at selected times. (C) Effect of cytochalasin D on  $\theta$  at selected times.  $*P < 0.05$ . [Color figure can be viewed at [wileyonlinelibrary.com](http://wileyonlinelibrary.com)]

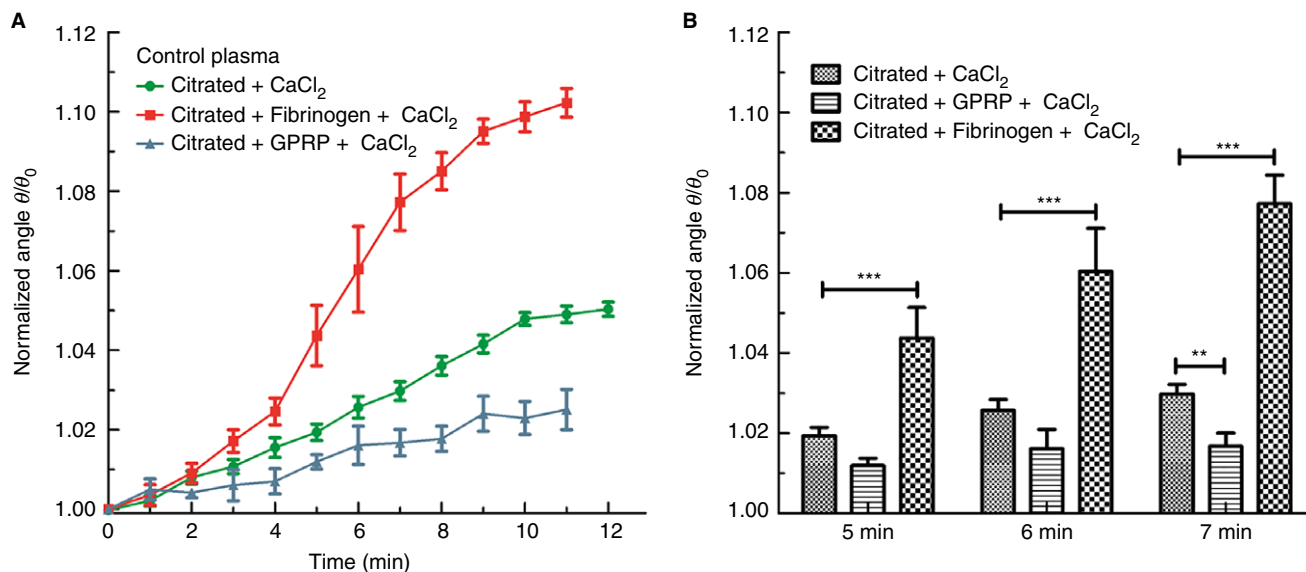


**Fig. 7.** (A) Tweezographs of citrated control plasma (FACT) with added  $\text{CaCl}_2$  and exposed to 0.9% saline (9 drops), fibrinogen (9 drops) or GPRP (9 drops). (B) Effect of fibrinogen and GPRP on  $\theta$  at 5, 6 and 7 min.  $**P < 0.01$ ,  $***P < 0.001$ . [Color figure can be viewed at [wileyonlinelibrary.com](http://wileyonlinelibrary.com)]



the induced amplitude. The time to achieve this 22-mm amplitude after the R time is reached is called the 'Kinetic time' or 'K time' in TEG, typically 1–3 min.

It is useful to compare our method and results with thromboelastographic tests. Our tweezergraph is analogous to the trace in TEG. Because our sample size is so small, 4  $\mu\text{L}$  compared with 360  $\mu\text{L}$  in TEG, the R time in our method is shorter than our first measurement, as indicated by Figs 5, 6 and 7. Short R times (80–140 s) can only be achieved in TEG using additive clotting factors ('TEG-ACT'). TEG needs R time plus K time (minimum 3 min TEG-ACT, maximum 13 min TEG) in order to obtain data with which to distinguish coagulation states. By contrast, our method can immediately detect differences in coagulation states induced by tissue factor (Fig. 6) or requires 5 min to detect the effects of pro-thrombotic agents such as fibrinogen (Fig. 7). The antithrombotic agent (e.g. GPRP) effects become pronounced in 7 min (Fig. 7).

The constant oscillatory shear that TEG, ROTEM and Sonoclot apply to a blood clot continuously disrupts the clot structure, leading to two competing processes: clotting and mechanical lysis. The trace obtained reflects the balance between these processes, with clotting dominating at early times and lysis dominating at later times. Importantly, it is unclear whether the lysis occurs in the bulk of the blood sample or at the surfaces of the pin or the cup. In contrast, our quasi-static technique is both non-contact and less destructive than the pin-and-cup methods; that is, it measures clotting throughout the blood sample without causing significant mechanical disruption. As a result, as can be seen in Figs 5, 6 and 7, our method does not artificially limit the clot firmness at some arbitrary time.

Three stages are identified in our graphical data (cf. Fig. 3D). The transition from Stage I and Stage II occurs when the fibrin network begins to connect the surface and bulk of the blood sample, leading to acceleration of the increase in firmness. By the end of Stage II, these connections fully populate the sample volume. The transition to Stage III is the manifestation of a cross-linked fibrin network, causing both slowing of the increase in firmness and permanent deformation, as observed in Fig. 4.

There are many improvements possible and many avenues of application open to us in the future. Of particular interest is the development of the oscillatory technique [15,16,19], which allows inference of viscosity and surface tension of whole blood in the liquid state within a few seconds. As the blood coagulates, this technique will yield complementary information about firmness, while simultaneously allowing inference of energy dissipation in the solid state.

Small sample volume and non-contact rapid measurement make the proposed method well suited for perioperative monitoring of blood coagulation in patients (especially pediatric patients) with coagulation disorders such as hemophilia [24] and thrombophilia [25], critical

care patients [26–29], and patients with other diseases that cause the coagulation system to dysfunction [30–34]. This method could be a valuable tool for transfusion guidance and analysis of stored blood products [35–37]. The small sample volume required opens up the possibility of whole-blood coagulation analysis of small children and home-use coagulation tests for patients with manageable diseases who are on antithrombotic medication [38].

## Addendum

D. B. Khismatullin and R. G. Holt were responsible for the study design and interpretation of the data. D. Luo and N. Gruver acquired the gel data. D. Luo acquired the blood data. R. G. Holt, D. B. Khismatullin, and D. Luo wrote the manuscript. D. B. Khismatullin, R. G. Holt, and D. Luo reviewed and revised the manuscript. All authors approved the final version of the manuscript.

## Acknowledgements

The authors thank J. Buell, H. Murad and H. Yu for help with blood experiments. This study has been financially supported by American Heart Association Grant-in-Aid 13GRNT17200013, US National Science Foundation grants 1438537 and 1438569, and in part by US National Institutes of Health grant 1U54GM104940-01, which funds the Louisiana Clinical and Translational Science Center. The funders had no role in study design, data collection and analysis, decision to publish or preparation of the manuscript.

## Disclosure of Conflict of Interests

D. B. Khismatullin and R. G. Holt have a patent 'PCT/US14/55559 - Apparatus, Systems & Methods for Non-Contact Rheological Measurements of Biological Materials' pending. The other authors state that they have no conflict of interest.

## References

- 1 Tripodi A, Mannucci PM. The coagulopathy of chronic liver disease. *N Engl J Med* 2011; **365**: 147–56.
- 2 Luddington RJ. Thrombelastography/thromboelastometry. *Clin Lab Haematol* 2005; **27**: 81–90.
- 3 Collins S, MacIntyre C, Hewer I. Thromboelastography: clinical application, interpretation, and transfusion management. *AANA J*. 2016; **84**: 129–34.
- 4 Saleem A, Blifield C, Saleh SA, Yawn DH, Mace ML, Schwartz M, Crawford ES. Viscoelastic measurement of clot formation: a new test of platelet function. *Ann Clin Lab Sci* 1983; **13**: 115–24.
- 5 Bolliger D, Seeberger MD, Tanaka KA. Principles and practice of thromboelastography in clinical coagulation management and transfusion practice. *Transfus Med Rev* 2012; **26**: 1–13.
- 6 Chen A, Teruya J. Global hemostasis testing thromboelastography: old technology, new applications. *Clin Lab Med* 2009; **29**: 391–407.

- 7 Lang T, von Depka M. Possibilities and limitations of thrombelastometry/thromboelastography. *Hamostaseologie* 2006; **26**: S21–9.
- 8 Carr ME Jr. In vitro assessment of platelet function. *Transfus Med Rev* 1997; **11**: 106–15.
- 9 Wang JS, Lin CY, Hung WT, O'Connor MF, Thisted RA, Lee BK, Karp RB, Yang MW. Thromboelastogram fails to predict postoperative hemorrhage in cardiac patients. *Ann Thorac Surg* 1992; **53**: 435–9.
- 10 Durila M, Kalincik T, Pacakova Z, Cvachovec K. Discard volume necessary for elimination of heparin flush effect on thromboelastography. *Blood Coagul Fibrinolysis* 2010; **21**: 192–5.
- 11 Chitlur M, Sorensen B, Rivard GE, Young G, Ingerslev J, Othman M, Nugent D, Kenet G, Escobar M, Lusher J. Standardization of thromboelastography: a report from the TEG-ROTEM working group. *Haemophilia* 2011; **17**: 532–7.
- 12 Marston PL. Shape oscillation and static deformation of drops and bubbles driven by modulated radiation stresses - theory. *J Acoust Soc Am* 1980; **67**: 15–26.
- 13 Tian YR, Holt RG, Apfel RE. Deformation and location of an acoustically levitated liquid-drop. *J Acoust Soc Am* 1993; **93**: 3096–104.
- 14 Tian Y, Holt RG, Apfel RE. A new method for measuring liquid surface-tension with acoustic levitation. *Rev Sci Instrum* 1995; **66**: 3349–54.
- 15 Tian Y, Holt RG, Apfel RE. Investigations of liquid surface rheology of surfactant solutions by Droplet Shape Oscillations - Theory. *Phys Fluids* 1995; **7**: 2938–49.
- 16 Tian Y, Holt RG, Apfel RE. Investigation of liquid surface rheology of surfactant solutions by droplet shape oscillations: Experiments. *J Colloid Interface Sci* 1997; **187**: 1–10.
- 17 McDaniel JG, Holt RG. Measurement of aqueous foam rheology by acoustic levitation. *Phys Rev E* 2000; **61**: R2204–7.
- 18 Ran W, Saylor JR, Holt RG. Improved particle scavenging by a combination of ultrasonics and water sprays. *J Aerosol Sci* 2014; **67**: 104–18.
- 19 Khismatullin DB, Nadim A. Shape oscillations of a viscoelastic drop. *Phys Rev E Stat Nonlin Soft Matter Phys.* 2001; **63**: 061508.
- 20 Solomon C, Schochl H, Ranucci M, Schlimp CJ. Can the viscoelastic parameter alpha-angle distinguish fibrinogen from platelet deficiency and guide fibrinogen supplementation? *Anesth Analg* 2015; **121**: 289–301.
- 21 Wehinger H, Klinge O, Alexandrakis E, Schurmann J, Witt J, Seydewitz HH. Hereditary hypofibrinogenemia with fibrinogen storage in the liver. *Eur J Pediatr* 1983; **141**: 109–12.
- 22 Canny J. A computational approach to edge detection. *IEEE Trans Pattern Anal Mach Intell* 1986; **8**: 679–98.
- 23 Tirtaatmadja V, Dunstan DE, Boger DV. Rheology of dextran solutions. *J Nonnewton Fluid Mech* 2001; **97**: 295–301.
- 24 Chitlur M, Young G. Global assays in hemophilia. *Semin Hematol* 2016; **53**: 40–5.
- 25 Jennings I, Cooper P. Screening for thrombophilia: a laboratory perspective. *Br J Biomed Sci* 2003; **60**: 39–51.
- 26 Herbstreit F, Winter EM, Peters J, Hartmann M. Monitoring of haemostasis in liver transplantation: comparison of laboratory based and point of care tests. *Anaesthesia* 2010; **65**: 44–9.
- 27 Jensen E, Andreasson S, Bengtsson A, Berggren H, Ekroth R, Larsson LE, Ouchterlony J. Changes in hemostasis during pediatric heart surgery: impact of a biocompatible heparin-coated perfusion system. *Ann Thorac Surg* 2004; **77**: 962–7.
- 28 Merlani PG, Chenaud C, Cottini S, Reber G, Garnerin P, de Moerloose P, Ricou B. Point of care management of heparin administration after heart surgery: a randomized, controlled trial. *Intensive Care Med* 2006; **32**: 1357–64.
- 29 Nascimento B, Al Mahoos M, Callum J, Capone A, Pacher J, Tien H, Rizoli S. Vitamin K-dependent coagulation factor deficiency in trauma: a comparative analysis between international normalized ratio and thromboelastography. *Transfusion* 2012; **52**: 7–13.
- 30 Loeffen R, Spronk HM, ten Cate H. The impact of blood coagulability on atherosclerosis and cardiovascular disease. *J Thromb Haemost* 2012; **10**: 1207–16.
- 31 Borissoff JI, Heeneman S, Kilinc E, Kassak P, Van Oerle R, Winckers K, Govers-Riemsag JW, Hamulyak K, Hackeng TM, Daemen MJ, ten Cate H, Spronk HM. Early atherosclerosis exhibits an enhanced procoagulant state. *Circulation* 2010; **122**: 821–30.
- 32 Marcucci R, Sofi F, Fedi S, Lari B, Sestini I, Cellai AP, Pulli R, Pratesi G, Pratesi C, Gensini GF, Abbate R. Thrombophilic risk factors in patients with severe carotid atherosclerosis. *J Thromb Haemost* 2005; **3**: 502–7.
- 33 Banga JD. Coagulation and fibrinolysis in diabetes. *Semin Vasc Med.* 2002; **2**: 75–86.
- 34 Noubouossie D, Key NS, Ataga KI. Coagulation abnormalities of sickle cell disease: relationship with clinical outcomes and the effect of disease modifying therapies. *Blood Rev* 2016; **30**: 245–56.
- 35 Karkouti K, McCluskey SA, Callum J, Freedman J, Selby R, Timoumi T, Roy D, Rao V. Evaluation of a novel transfusion algorithm employing point-of-care coagulation assays in cardiac surgery: a retrospective cohort study with interrupted time-series analysis. *Anesthesiology* 2015; **122**: 560–70.
- 36 Cardigan R, Van der Meer PF, Pergande C, Cookson P, Baumann-Baretti B, Cancelas JA, Devine D, Gulliksson H, Vassallo R, de Wildt-Eggen J. Coagulation factor content of plasma produced from whole blood stored for 24 hours at ambient temperature: results from an international multicenter BEST Collaborative study. *Transfusion* 2011; **51**(Suppl. 1): 50S–7S.
- 37 Scott E, Puca K, Heraly J, Gottschall J, Friedman K. Evaluation and comparison of coagulation factor activity in fresh-frozen plasma and 24-hour plasma at thaw and after 120 hours of 1 to 6 degrees C storage. *Transfusion* 2009; **49**: 1584–91.
- 38 Salmela B, Joutsu-Korhonen L, Armstrong E, Lassila R. Active online assessment of patients using new oral anticoagulants: bleeding risk, compliance, and coagulation analysis. *Semin Thromb Hemost* 2012; **38**: 23–30.